Review

Palladium-Based Catalysts as Electrodes for Direct Methanol Fuel Cells: A Last Ten Years Review

Juan Carlos Calderón Gómez, Rafael Moliner and Maria Jesus Lázaro *

Instituto de Carboquímica (CSIC), Miguel Luesma Castán 4, Zaragoza 50018, Spain;
jccalderon@icb.csic.es (J.C.C.G.); rmoliner@icb.csic.es (R.M.)
* Correspondence: mlazaro@icb.csic.es; Tel.: +34-976-733-977

Abstract: Platinum-based materials are accepted as the suitable electrocatalysts for anodes and cathodes in direct methanol fuel cells (DMFCs). Nonetheless, the increased demand and scarce world reserves of Pt, as well as some technical problems associated with its use, have motivated a wide research focused to design Pd-based catalysts, considering the similar properties between this metal and Pt. In this review, we present the most recent advancements about Pd-based catalysts, considering Pd, Pd alloys with different transition metals and non-carbon supported nanoparticles, as possible electrodes in DMFCs. In the case of the anode, different reported works have highlighted the capacity of these new materials for overcoming the CO poisoning and promote the oxidation of other intermediates generated during the methanol oxidation. Regarding the cathode, the studies have showed more positive onset potentials, as fundamental parameter for determining the mechanism of the oxygen reduction reaction (ORR) and thus, making them able for achieving high efficiencies, with less production of hydrogen peroxide as collateral product. This revision suggests that it is possible to replace the conventional Pt catalysts by Pd-based materials, although several efforts must be made in order to improve their performance in DMFCs.

Keywords: palladium catalysts; direct methanol fuel cells; methanol oxidation; oxygen reduction; non-Pt content

1. Introduction

Direct methanol fuel cells (DMFCs) are alternative energy sources being employed in portable and electronic devices, considering the evident increase of energy price during the last years. Methanol is the fuel used in these devices, which has been recognized due to its high energy density and its easy handling [1]. Therefore, many research articles have been devoted to the study of them, in order to promote their entrance into the market. However, the high price of DMFCs is the main factor avoiding its commercialization, in spite of the progress in prototypes and mass production design, which does not have a direct relationship with the materials costs [2]. The high cost of these devices comes from the use of platinum and platinum alloys for methanol oxidation and oxygen reduction, the electrochemical reactions performed on anode and cathode, respectively. Some possible alternatives focused in the use of low platinum contents have been studied [3], particularly in the case of the cathode, suggesting materials including heat treated transition metals macrocycles [4,5], ruthenium chalcogenides [6,7] and palladium alloys [7,8]. Particularly, replacement of platinum and its alloys in the anode require more investigation, being the best solution the use of non-platinum catalysts in alkaline electrolytes [9,10].

Within this context, palladium has been suggested for substituting the platinum in anodes and cathodes of DMFCs because of the similarities between these metals, as well as the major abundance and low cost of Pd [11]. Mining sources of palladium are more abundant than those for Pt, a fact that makes Pd cheaper ($654.1 per oz.) than Pt ($1796.9 per oz.) [12]. Furthermore, in the case of the anode, palladium has displayed high tolerance towards CO poisoning [13] and high catalytic activity for alcohols oxidation in alkaline medium [12,14,15]. Regarding the cathode, Pd-based catalysts have also arisen as an alternative to perform the oxygen reduction reaction (ORR), especially if this metal is combined with other transition metals, which induce changes in the Pd electronic structure, and thus, increasing its activity [16].

In this work, a review of the progress of Pd-based catalysts for both anodes and cathodes in DMFCs is presented, considering two categories: carbon-supported and non-carbon-supported catalysts. The effect of second metals and novel supports in the catalytic activity is discussed, in order to explain why these Pd catalysts could be suggested as electrodes for direct methanol fuel cells.

2. Methanol Oxidation on Pd-Based Catalysts

2.1. Carbon-Supported Pd-Alloys

The role of carbon materials as support for catalysts in all the categories of polymer electrolyte membrane fuel cells is well known, and is related with different factors: (1) enhancement of high electroactive area, caused by a better dispersion of nanoparticles [17]; (2) improved electroactive species diffusion through the porous structure of carbon support [17]; and (3) promotion of the electronic transfer, either for the presence of surface functional groups or the decrease in Fermi level of the catalysts [18]. Therefore, a way for increasing the activity of catalysts is upgrading the electrical and morphological properties of carbon supports, a fact applied for both Pt-based and non Pt-based electrocatalysts. In this sense, graphene has been suggested as a good alternative to support Pd nanoparticles in order to improve the performance of anodic catalysts during the methanol oxidation reaction (MOR). Zhang and co-workers have found enhanced electrocatalytic activity for methanol oxidation when these kinds of materials are employed as anode catalysts, which was attributed to the large electrochemically active surface area (ECSA) generated by the large amount of active edge sites present in the graphene. These sites are able to anchor the Pd nanoparticles and modify the electronic properties of them, obtaining high currents in the forward scan and thus improved efficiency toward the production of CO_2 as principal product during the methanol oxidation [19]. In other work [20], the synthesis of ultrafine Pd nanoparticles (NPs) supported on N- and S-modified graphenes was reported. In this case, the effects caused by the high surface area of graphene were represented in the increased electrocatalytic performance during the methanol electro-oxidation, as well as the catalytic stability in comparison with the corrosion resistance displayed by Pd nanoparticles supported on both, undoped graphene and Vulcan XC-72R carbon black. Another example of the remarkable benefits in the catalytic activity caused by graphenes can be seen in a recent work reported by Zhang et al. [21], which prepared hybrid composites between graphitic carbon nitride and reduced graphene oxides as support for Pd nanostructures. These materials displayed high forward peak current densities, which were explained from: (1) the large ECSA; (2) the presence of planar groups that modified interactions between the support and the nanoparticles; and (3) the long-term stability of the composites. In fact, the current densities overcame those observed for Pd nanoparticles supported on reduced graphenes and a commercial Pd catalyst supported on activated carbon. Table 1 displayed some electrochemical parameters determined for catalysts supported on graphenes.

Table 1. Electrochemical properties of Pd catalysts supported on graphenes, doped graphenes, RGO, reduced graphene oxide.

Catalyst	Electrochemical Parameter			Reference
	Onset Potential (V vs. RHE)	Anodic Peak Potential (V vs. RHE)	Anodic Peak Current (mA mg^{-1} Pd)	
Pd/CNNF-G	0.420	0.800	1780	
Pd/C$_3$N$_4$-RGO	0.450	0.800	1550	
Pd/RGO	0.570	0.810	860	[19]
Pd/CNT	0.570	0.850	700	
Pd/AC	0.580	0.870	550	
Pd/C$_3$N$_4$	0.780	0.870	80	
Catalyst	Onset Potential (V vs. RHE)	Anodic Peak Potential (V vs. Hg/HgO)	Anodic Peak Current (mA cm^{-2})	Reference
Pd/NS-G	0.472	0.880	12.5	
Pd/G	0.600	0.880	7	[20]
Pd/C	0.520	0.890	5.6	

Generally, Pd-based catalysts are supported on carbon blacks, bearing in mind its high conductivity and low cost. An example of these catalysts are the Pd-M alloys (M = Ag, Ni, Rh, and Au), which have displayed different activities towards the methanol oxidation. Incorporation of Ag into the crystalline structure of Pd is one of the most studied non-Pt alloys, because of its high performance. Yin et al. [22] reported upper activities for Pd-Ag catalysts supported on Vulcan XC-72 carbon black, especially at Pd:Ag atomic ratios close to 65:35 and 46:54. In other work, Wang et al. [23] supported Pd-Ag nanoparticles on carbon blacks, varying the Ag content and finding the Pd:Ag 1:1 atomic ratio as the most efficient composition in terms of electrocatalytic activity in alkaline medium. Ag induced a decrease in the methanol oxidation onset potential (0.436 V vs. RHE), in comparison with that observed for a Pd/C catalyst (0.536 V vs. RHE). Furthermore, the authors reported that addition of Ag promoted the easy removal of CO$_{ads}$, increasing the number of active sites able to adsorb and oxidize methanol. The causes associated with the activity enhancement by Ag presence in the alloy were explained from a displacement in the d-band center of Pd, affecting the electronic properties of this metal and the activation of water at lower potentials in comparison with those required for Pd, which participates in the oxidation of CO$_{ads}$. Although the authors demonstrated that presence of Ag in these carbon black-supported materials is profitable for the activity of Pd, the major increase in the activity of this noble metal was achieved for the Pd-Ag alloy supported on carbon nanotubes (CNTs). They demonstrated that catalysts supported on CNTs possessed bigger electroactive surface and better catalytic activity than Pd-Ag/C Vulcan XC-72R, possibly because of high specific surface area and big pore volume of CNTs. The Pd-Ag/CNTs exhibited more remarkable current densities during the electrochemical oxidation of methanol than Vulcan XC-72R-supported catalysts. Reduced graphene oxides have also been used as supports for Pd-Ag nanoparticles, displaying good performances, particularly for the oxidation of the intermediates generated during the MOR. It is well known that the novel properties of graphenes are principally related with the elevated conductivity caused by its graphite plane structure [24]. A work reported by Li and co-workers [25] showed an improved oxidation of intermediates on Pd-Ag/ reduced graphene oxide (RGO), by means of the oxidation peaks generated during the forward (I_f) and reverse scans (I_b), which appeared in the methanol oxidation cyclic voltammetries. The oxidation of these chemisorbed intermediates was efficiently performed in the backward scan, as they are not totally oxidized during the forward scan. The highest ratio between these forward and backward currents was displayed by the catalyst Pd-Ag (1:1.5)/RGO, indicating a high conversion of methanol to CO$_2$ with a low production of intermediates. However, the authors considered Pd-Ag (1:1)/RGO as the best catalyst, because of the highest current densities displayed during the methanol oxidation. As mentioned above, the improved performance of these graphene-supported materials was attributed to the presence of Ag and its synergistic effect with Pd for methanol electro-oxidation. In general, the role of Ag, with independence of the employed carbon

support, is related to its oxophilic character, which promotes the OH_{ads} adsorption, making easy the methanol dehydrogenation and CO_{ads} oxidation steps.

$$CH_3OH \rightleftharpoons CH_3OH_{ads} \tag{1}$$

$$CH_3OH_{ads} \rightarrow CO_{ad} + 4H^+ + 4e^- \tag{2}$$

$$H_2O \rightarrow OH_{ad} + H^+ + e^- \tag{3}$$

$$CO_{ad} + OH_{ad} \rightarrow CO_2 + H^+ + e^- \tag{4}$$

In this mechanism, after adsorption of methanol (Equation (1)), its deprotonation is carried out (Equation (2)) forming CO_{ad} which is oxidized by OH_{ad} (produced from water dissociation in Equation (3)), generating CO_2 and liberating the catalytic surface (Equation (4)). As demonstrated in a recent differential electrochemical mass spectrometry (DEMS) study [26], these factors produce obtaining large CO_2 current efficiencies at low oxidation potentials and lower potentials for CO_{ads} oxidation, as well as a displacement of the methyl formate forming potential towards more positive potentials, guaranteeing the complete oxidation of methanol. The effects attributed to graphene are related to high surface area, high electrical conductivity, upgraded electronic transference and the obtaining of more small and stable metal nanoparticles [25]. Table 2 displays some electrochemical performances and parameters obtained during the electrochemical oxidation of methanol on carbon-supported Pd-Ag catalysts.

Table 2. Electrochemical properties of Pd-Ag catalysts supported on different carbon materials.

Catalyst	Electrochemical Parameter			Reference
	Onset Potential (V vs. RHE)	Anodic Peak Potential (V vs. RHE)	Anodic Peak Current (mA mg^{-1} Pd or Pt)	
Pd/C	0.545	0.915	210.5	
Pd$_{80}$Ag$_{20}$/C	0.475	0.904	691.6	
Pd$_{65}$Ag$_{35}$/C	0.435	0.865	629.6	[22]
Pd$_{46}$Ag$_{54}$/C	0.475	0.855	453.4	
Pt/C TKK	0.475	0.925	689.3	
Catalyst	**Onset Potential (V vs. RHE)**	**Anodic Peak Potential (V vs. RHE)**	**Anodic Peak Current (mA cm^{-2})**	**Reference**
Pd/C	0.536	0.928	0.557	
Pd-Ag(2:1)/C	0.446	0.886	0.635	
Pd-Ag(1:1)/C	0.436	0.856	0.678	[23]
Pd-Ag(1:1)/CNTs	0.436	0.886	0.950	
Pd-Ag(1:1.5)/C	0.446	0.856	0.707	
Catalyst	**Anodic Peak Potential (V vs. RHE)**	**Anodic Peak Current (mA mg^{-1} Pd)**	**Ratio Between Forward and Backward Anodic Currents**	**Reference**
Pd/C	0.915	311	1.41	
Pd-Ag(1:1)/GO	0.865	225	1.50	
Pd-Ag(1.5:1)/RGO	0.915	334	1.42	[25]
Pd-Ag(1:1)/RGO	0.875	630	3.15	
Pd-Ag(1:1.5)/RGO	0.895	585	6.55	
Pd-Ag(1:1)/RGO-SB	0.870	545	1.48	

Carbon black-supported Pd-Ni is another widely reported alloy useful for carrying out the methanol oxidation. Different studies have demonstrated that presence of NiO in Pd catalysts can reduce the onset potential for the MOR, as well as increase the oxidation current densities [27]. It seems that nickel produces a similar effect to that for ruthenium in terms of the capacity to form OH_{ads} at lower potentials than Pd. Furthermore, Ni can induce changes in the electronic properties of Pd, similarly to the silver effect cited above [28]. These facts are reflected in the elevated currents associated with the hydrogen adsorption/desorption process and the resistance towards the carbonaceous intermediates poisoning during the methanol oxidation [29]. In order to elucidate the origin of the improved activity

in Pd-Ni catalysts supported on carbon blacks, Amin et al. determined the Ni surface coverage in these alloys, trying to correlate the presence of Ni oxides and hydroxides with the methanol oxidation current densities [30,31]. The authors found enhanced current densities at big Ni coverages, due to the Ni oxophilic character and its capacity to generate adsorbed Ni hydroxides at low potentials. Another conclusion from these works was the ability of the NiOH and NiOOH for oxidizing the CO_{ads} generated during the methanol oxidation, which occupies active Pd sites. Besides the incorporation of oxygenated species by Ni, it has also been suggested the appearance of some defects on palladium crystalline lattice, with a major activity towards the methanol oxidation [32]. Atomic ratio between Pd and Ni also played a key role in the activity of these carbon black-supported catalysts, as demonstrated by Calderon et al. in a recent work [33]. They synthesized Pd-Ni catalysts supported on chemically treated carbon blacks, which contained surface oxygen and nitrogen groups. The metal contents of these catalysts was close to 25 wt %, whereas the studied Pd:Ni atomic ratios were near 1:1 and 1:2. Although no evident effects related to the presence of O- and N-surface functional groups were observed, these catalysts exhibited a higher CO poisoning tolerance than that observed for a Pd/C catalyst, which was explained from the increased amount of OH_{ads} formed on surface Ni atoms, while the methanol oxidation produced higher current densities in the catalysts with Pd:Ni = 1:2, in comparison with current densities generated with the catalysts with the atomic ratio close to 1:1 and the catalysts without any content of Ni (catalyst Pd/C), being this fact a proof of the beneficial effects of Ni in this reaction. Regarding other novel carbon materials as supports for Pd-Ni catalysts, Singh et al. [34] synthesized PdNi alloys supported on multi-walled carbon nanotubes (MWCNTs), finding remarkable activities toward the methanol oxidation, which were explained from the increased electroactive area of these composites, promoted by the use of MWCNTs and the electronic properties of the alloys, as described above. All of the authors coincided in the change of these electronic properties, also promoted by Ni oxides and hydroxides, being crucial factors for enhancing the electrochemical activity of the catalysts.

Other authors have suggested the doping of MWCNTs, as a plausible alternative for improving the activity, using for instance MnO_2 to cover the surface of carbon materials [35]. The presence of MnO_2 upgraded the electrocatalytic activity of Pd/MWCNTs and the tolerance to carbonaceous species poisoning, considering the high current values in the forward anodic peak current density (I_f). This value indicated a more effective removal of the poisoning species from the catalyst surface, oxidizing them to carbon dioxide. The authors suggested that the better activity for the Pd-MnO_2/MWCNT catalyst could be explained from the synergetic effect between Pd and MnO_2, promoting the adsorption of OH_{ad} species able to convert the poisoning species to CO_2. Table 3 present some catalytic parameters determined for the MOR performed on Pd-Ni catalysts supported on carbon materials.

Rh is another metal recently proposed to be alloyed with Pd. This metal is known for applications as exhaust systems in automobiles [36] and CO-tolerant electrode for the oxidation of H_2 in high temperature-proton exchange membrane fuel cells if hydrogen comes from a gas reformate process [37]. Studies related with the ethanol oxidation on Pt-Rh alloys in acidic and alkaline media have also been reported, displaying good methanol conversions to CO_2 [38–41], and generating efficiencies explained from the high Rh oxophilicity. About the methanol oxidation, Jurzinsky and co-workers [42] prepared Pd-Rh catalysts supported on carbon blacks, observing lower onset potentials and higher mass current densities than those exhibited by a Pd/C catalyst. The principal properties conferring to this Pd-Rh a high catalytic activity are related with: (1) capacity to form OH_{ads} at low potential; and (2) high stability of these OH_{ads}. The authors suggested that addition of Rh increased the tolerance of Pd towards the poisoning caused by different intermediates and CO. By means of some DEMS experiments, they also demonstrated that Pd-Rh/C catalysts can increase the efficiency in the oxidation of methanol to CO_2. DMFCs single test demonstrated enhanced power densities when these catalysts were used as anodes, in comparison with the performances obtained with Pd/C and Pt/C as anodes. The behavior of Pd-Rh alloys supported on graphenes meant an enhancement of the methanol oxidation currents, as was

reported by Hsieh et al. [43]. The enhanced catalytic activity was attributed to the well-dispersed nanoparticles supported on the graphenes, resulting in a high active surface area and more active sites than those formed when the alloys are supported on carbon blacks. Another important advantage for the use of graphenes as support could be related with the major conductivity of this material due to their graphite plane structure.

Table 3. Electrochemical properties of Pd-Ni catalysts supported on different carbon materials.

Catalyst	Electrochemical Parameter			Reference
	Onset Potential (V vs. RHE)	Anodic Peak Current (mA cm^{-2})	–	
Pd/C	0.555	14	–	
Pd-NiO(8:1)/C [a]	–	51	–	
Pd-NiO(6:1)/C [a]	–	61	–	[27]
Pd-NiO(4:1)/C [a]	–	74	–	
Pd-NiO(2:1)/C	0.535	63	–	
Pt/C	0.525	18	–	

Catalyst	Anodic Peak Potential (V vs. RHE)	Anodic Peak Current (mA cm^{-2})	–	Reference
Pd-Ni(1:1)/C	0.914	7,64	–	[30]
Pd-Ni(1–5wt %)/MWCNTs	0.969	341,68	–	[34]

Catalyst	Onset Potential (V vs. RHE)	Anodic Peak Potential (V vs. RHE)	Anodic Peak Current (mA cm^{-2})	Reference
Pd/C	0.611	1.006	1.41	
Pd-Ni(1:1)/C	0.421	0.941	1.50	[32]
Pt/C	0.441	1.006	1.48	

Catalyst	Onset Potential (V vs. RHE)	Anodic Peak Current (mA cm^{-2})	Reference
Pd-Ni/CB 1:1	0.452	0.912	
Pd-Ni/CBO 1:1	0.556	0.397	
Pd-Ni/CBN 1:1	0.511	0.536	
Pd-Ni/CB 1:2	0.498	1.100	[33]
Pd-Ni/CBO 1:2	0.458	1.126	
Pd-Ni/CBN 1:2	0.551	0.815	
Pd/C 1:1	0.600	0.310	

[a] Data not provided by the authors.

Cerium is another metal tested as a component of palladium alloys. A work reported by Alvi and co-workers [44] reported the synthesis of Pd-Ce nanoparticles supported on carbon nanofibers synthesized by electrospinning. They employed these materials as catalysts for the methanol oxidation, obtaining materials with crystalline structure and highly-dispersed Pd-Ce nanoparticles on the carbon nanofibers surface. Regarding the catalytic activity, these materials displayed an acceptable efficiency toward the methanol oxidation, with enhanced current densities depending of the increase in the methanol concentration. Regarding the use of Pd-Au catalysts, recently He and co-workers reported the deposition of Au@Pd core-shells on reduced graphene oxide, synthesized by chemical reduction in presence of cetyltrimethylammonium chloride and iodide ions [45]. This catalyst showed high catalytic activity and tolerance to carbonaceous species poisoning generated during the methanol oxidation, overcoming those observed for Pd nanoparticles supported on reduced graphene oxide and commercial Pd/C in alkaline media. This behavior was explained from the strong interactions between reduced graphenes and Au@Pd nanostructures. Some electrochemical properties reported by different authors, regarding to different palladium alloys are reported in Table 4.

Table 4. Electrochemical properties of Pd-alloys supported on different carbon materials.

| Catalyst	Electrochemical Parameter		Reference
	Onset Potential (V vs. RHE)	Anodic Peak Current (mA mg^{-1} Pd)	
Pt/C (HiSPEC^{TM} 3000)	0.475	669.9	
Pd/C	0.585	543.8	
Rh/C	0.504	177.6	[42]
PdRh$_3$/C	0.500	369.2	
PdRh/C	0.445	933.9	
Pd$_3$Rh/C	0.497	955.7	
Catalyst	**Onset Potential (V vs. RHE)**	**Anodic Peak Current (mA mg^{-1} Pd)**	**Reference**
Pd/GO	0.260	73	
Pd$_{75}$Rh$_{25}$/GO	0.280	100	[43]
Pd$_{50}$Rh$_{50}$/GO	0.370	35	
Pd$_{25}$Rh$_{75}$/GO	0.310	31	
Catalyst	**Onset Potential (V vs. RHE)**	**Anodic Peak Current (mA mg^{-1} Pd)**	**Reference**
Pd/C	0.510	190	
Pd/MWCNTs	0.510	285	[35]
Pd-MnO$_2$/MWCNTs	0.460	420	
Catalyst	**Onset Potential (V vs. RHE)**	**Anodic Peak Current (mA cm^{-2})**	**Reference**
Au@Pd/RGO	0.500	28	
Pd/RGO	0.700	4	[45]
Pd/C	0.640	10	

In terms of the palladium amount employed in some alloys, the mentioned works indicate that Pd-Rh materials generate the highest performances in terms of the current densities produced during the methanol oxidation. Particularly, the work of Jurzinsky and co-workers [42] highlights the catalyst PdRh/C, supported on Vulcan carbon black XC-72R, with a metal content of 20 wt % and an atomic ratio Pd:Rh close to 1:1. This material exhibited the highest current density (close to 1 A mg^{-1} Pd), being one of the most promising catalysts because of its low Pd content. Silver seems to be other metal with a remarkable behavior due to the formation of OH$_{ads}$, which play a key role in the oxidation of methanol. According to the work of Yin et al. [22], the better performance was showed for the catalyst Pd$_{80}$Ag$_{20}$/C, also supported on Vulcan carbon black XC-72R, with current densities close to 700 mA mg^{-1} Pd, although in this case, higher metal and Pd contents (close to 30 wt % and Pd:Ag of 80:20) were necessary for achieving this performance. Therefore, it is possible to postulate rhodium as the suitable metal to be alloyed with Pd, in carbon-supported catalysts for anodes in DMFCs.

*2.2. Non Carbon-Supported Pd-Alloys*

Although carbon materials have been traditionally used as supports for catalysts in low temperature fuel cells, some problems associated with its corrosion suggest the necessity for design novel supports able to supply the properties of carbon materials. In the carbon corrosion process, carbon surface (C$_s$) is oxidized, forming intermediates and electrons (Equation (5)) [46]:

$$C_s \rightarrow C_s{}^+ + e^- \tag{5}$$

These electroactive species are susceptible to be hydrolyzed (Equation (6)):

$$C_s + H_2O \rightarrow C_sO + 2H^+ + e^- \tag{6}$$
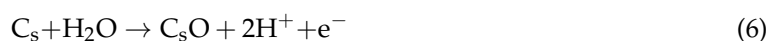
The final step of the corrosion process is the formation of carbon dioxide (Equation (7)):

$$2C_sO + H_2O \rightarrow C_sO + CO_{2(g)} + 2H^+ + e^- \qquad (7)$$
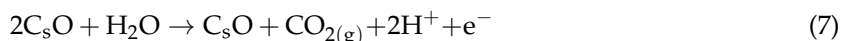
Accordingly, some possible alternatives for substituting the carbon materials have been explored, looking for improving the activity of electrodes in fuel cells. For instance, Pd nanoparticles supported on Ni foam, with different Pd contents (Pd-2-Ni and Pd-4-Ni) were synthesized by galvanic replacement of Ni with $PdCl_4^{2-}$ and $PdCl_6^{2-}$ [47]. The activities of these materials were better than that exhibited by a commercial Pd/C, possibly due to the re-arrangement of Pd atoms and their improved utilization, which depended of the employed precursor during the synthesis. Moreover, a major exposition of Ni atoms probably promoted the oxidation of methanol, considering the above-mentioned role of this metal in this reaction.

On the other hand, titanium oxides have demonstrated attractive properties as low cost, commercial availability and high stability [48–50]. Since TiO_2 is recognized by its semiconductor properties, it is important to improve its electronic conductivity by means of the introduction of electron-donor dopants [51]. Nonetheless, there are few reports about the use of TiO_2 as support for Pd-based catalysts. In this sense, some researchers attempted to deposit Pd nanoparticles on TiO_2 nanotubes, finding remarkable catalytic activities in comparison with those observed for a pure Pd electrode and those Pd-nanostructures supported on TiO_2 nanoparticles [52]. The authors justified this improved activity from the well-dispersed nanoparticles on titanium tubes, which possessed a small diameter, thus promoting the obtaining of high specific surface areas. In these catalysts, the CO poisoning was also diminished, possibly due to some modifications in the Pd electronic structure induced by TiO_2, improving the CO oxidation process. In other work, Hosseini et al. [53] prepared Pd nanoparticles supported on an auto-assembled TiO_2 nanotubes/titanium support with a highly porous structure. This composite favored the diffusion of electroactive species toward the Pd nanoparticles, enhancing the methanol oxidation currents and conferring high stability. Another important property displayed by this support was its low electrochemical charge transfer resistance during the methanol oxidation activation stage.

Regarding the Pd-alloys supported on these TiO_2 supports, the most recent progresses are related with the presence of Ni and Ag on them, in agreement with some reports from Ju and co-workers. In the case of nickel [54], they supported Pd-Ag nanoparticles on TiO_2 nanotubes by surface reductive deposition of $PdCl_2$ and $NiSO_4$ on TiO_2 nanotubes. Large surface area and porous structure was observed for the Ti supports, improving the dispersion of Pd-Ni nanoparticles, whereas the electrochemical characterization exhibited high hysteresis peaks in the forward and backward scans, being this fact a proof of the high efficiency for the methanol intermediates oxidation. Again, the authors suggested the synergistic effect between Pd-Ni alloy and the TiO_2 nanotube support as responsible of the improved activity of these materials. On the other hand, the Pd-Ag alloys [54] showed remarkable electrocatalytic activity with high tolerance to the poisoning when tested towards the methanol electrochemical oxidation, although in this case, no hysteresis peaks were observed. Moreover, the dispersion of Pd-Ag nanoparticles was worse than that of Pd-Ni nanoparticles. In a recent work, Cao et al. [55] prepared nanoporous catalysts conformed by Pd, CuO and TiO_2, following a chemical dealloying process of amorphous Cu-Pd alloy ribbons in 5 M hydrochloric acid solution. Then, they deposited TiO_2 nanoparticles, forming composites as np-Pd/CuO/160TiO$_2$ (with 160 as the TiO_2 moles present in the composite), which exhibited high activity toward the methanol oxidation and enhanced current densities (close to 2.86 mA cm^{-2}). The improved activity of this material was attributed to the ability of TiO_2 nanoparticles to form oxygen species able to promote the oxidation of methanol poisoning intermediates. Furthermore, these materials presented an outstanding long-term stability. The effect of some TiO_2 supports in the catalysis of methanol oxidation can be verified through the kinetic parameters shown in Table 5.

Table 5. Kinetic parameters for the methanol oxidation on Pd-based catalysts supported on TiO_2 materials.

Catalyst	Electrochemical Parameter		Reference
	Onset Potential (V vs. RHE)	Anodic Peak Current (A)	
Pd (pure)	0.22	1.0	
Pd/TiO$_2$ (nanoparticles)	0.22	4.5	[52]
Pd/TiO$_2$ (nanotubes)	0.23	9.0	
Catalyst	Onset Potential (V vs. RHE)	Anodic Peak Current Density (mA cm^{-2})	Reference
np-Pd/CuO/80TiO$_2$	0.55	1.5	
np-Pd/CuO/160TiO$_2$	0.51	2.8	
np-Pd/CuO/240TiO$_2$	0.55	1.4	[55]
np-Pd/CuO	0.60	0.8	
np-Pd	0.55	0.7	

From the works described above, it is possible to conclude that novel supports as nickel foams and TiO_2 nanotubes offer good properties to increase the performance of palladium nanoparticles toward the MOR. Basically, Ni foam facilitates the formation of OH_{ads}, and thus, increases to the CO poisoning tolerance, as reported by Niu et al. [47], who employed a surface metal loading of Pd close to 1 mg cm^{-2}, obtaining current densities close to 180 mA mg^{-1} Pd. In the case of the TiO_2-supported catalysts, the nanotube structure displayed the better performance [52] as a consequence of the improved diffusion of electroactive species toward the nanoparticles. The main drawback of this material is related with the low conductivity of this support, a fact that encourages the researches toward the doping of this support with other metals in order to increase its conductivity.

3. Oxygen Reduction on Pd-Based Catalysts

3.1. Carbon-Supported Pd-Alloys

Essentially, it is possible to consider similar problems in the cathode in comparison with those observed for the anode, in terms of cost issues and activity/technical limitations. This reaction starts with the adsorption of oxygen on catalyst surface, but different pathways can be followed (see Figure 1), as the direct forming process of water, which implies the maximum production of electrons (four electrons). However, production of hydrogen peroxide is also possible, a fact that results in the increase of the corrosive operation conditions of the DMFCs and the decrease in their performance, considering the production of two electrons during the reduction from molecular oxygen to H_2O_2 [56].
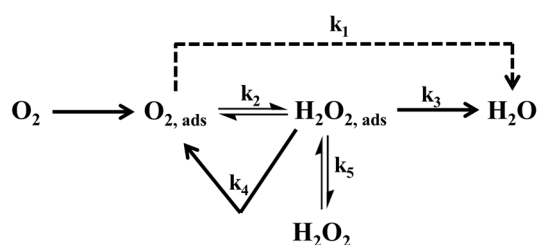
Figure 1. Mechanism and pathways for the oxygen reduction reaction.

Other typical drawbacks in the cathodes of direct methanol fuel cells are related with the adsorption of oxygen on the catalytic nanoparticles, the kinetics associated with the O-O cleavage, the crossover of methanol and the reduction of surface metal oxides once the oxygen has been transformed in water [56]. In this sense, significant progress has been achieved by researchers studying the

ORR reaction on ruthenium chalcogenides [6,7,57], heat-treated macrocyclic compounds of transition metals [58–60], and palladium-based catalysts [8,61,62]. Regarding the catalyst supported on carbon materials different than carbon blacks, Zheng et al. supported palladium nanoparticles on carbon nanofibers and activated carbons in order to determine the influence of the carbon support on the ORR [63]. They found that this reaction is controlled by surface phenomena if the catalyst is supported on activated carbons, whereas diffusion of electroactive species is the factor controlling this reaction if the catalyst is supported on carbon nanotubes. Furthermore, carbon supports played a crucial role in the onset potentials for the ORR, being the Pd nanoparticles supported on activated carbons which displayed the most negative onset potential (0.50 V vs. RHE in acid media), whereas the catalysts supported on carbon nanofibers displayed values close to 0.70 V for the fishbone carbon nanofibers and 0.72 V for the platelet carbon nanofibers. In other study, Chakraborty and co-workers synthesized spherical and rod-like shapes nanosized Pd particles supported on multiwall carbon nanotubes (MWCNTs) [64] employing an electroless procedure. The results of this study indicated that these MWCNT-supported nanoparticles have remarkable catalytic activity towards the oxygen reduction, controlled by the surface morphology and coverage of particles on the carbon nanotubes, with a reaction mechanism that promoted the formation of hydrogen peroxide. The most important facts related with the electrocatalytic activity of these materials were related with the positive onset potentials for the ORR, the high stability of the catalysts as well as the definition of several peaks, which indicated the production of H_2O_2 in the first step of the ORR mechanism. Subsequently, this hydrogen peroxide is reduced to H_2O (second stage of the mechanism). Following the line of the shaped-controlled synthesis of Pd nanoparticles, Lusi et al. [65] recently reported the preparation of Pd nanocubes supported on Vulcan carbon black, finding several sizes such as 30, 10 and 7 nm. The authors assessed the electrocatalytic activity of these materials towards the ORR in alkaline media, and observed a four-electron pathway with the transfer of the first electron to adsorbed O_2 as the rate-limiting step. Furthermore, the specific activity of these nanocubes overcame that of the spherical Pd nanoparticles, finding a correlation between the enhanced activities and the increase of the particle size. Although this study demonstrated the achievement of high efficiencies in the ORR with big particle sizes, another recent research also suggested that it is possible to obtain high performances with ultra small thiolate-protected Pd nanoclusters [66], with ORR onset potential of −0.09 V (vs. Ag/AgCl) in alkaline media and improved durability. The authors verified the effects of thiolated ligands removing, finding a more positive onset potential (close to −0.02 V) and higher mass activity than that of a Pt/C catalyst, a fact explained from an activation of the nanoclusters after the thiolated ligands removing process.

Another study about the catalysis of the ORR in acid and alkaline media on Pd nanoparticles supported on MWCNTs was reported by Jukk and co-workers [67]. In this work, they employed Nafion® and polyvinylpyrrolidone as surfactants during the synthesis procedure. These surfactants conditioned the final performance of the materials, with the Nafion®-synthesized material exhibiting higher current densities and more positive onset potentials during the ORR tests, whereas the catalyst prepared in presence of polyvinylpyrrolidone displayed an equivalent behavior to that of a bulk Pd electrode. The authors suggested that these surfactants modified the amount and morphology of the as-formed Pd oxides, altering the adsorption oxygen and the reaction pathway.

Regarding the Pd alloys, Pd-Ni supported on carbon blacks exhibited high activity, as shown by Li and co-workers, who found high ORR activities, even better than those produced for a Pd/C catalyst [68]. The number of transferred electrons was also calculated, and it was demonstrated that a high content of surface Ni atoms promote the yielding of H_2O_2. This behavior was modified with a heat treatment at 800 °C, which induced the segregation of Pd atoms to the nanoparticles surface, generating a major number of produced electrons and thus, promoting the formation of water and increasing the current densities. Ramos-Sánchez et al. [69] also synthesized these nanoparticles supported on Vulcan carbon black by a borohydride reduction in THF. These materials developed power densities close to 120 mW cm^{-2} when used as cathodes in a direct methanol fuel single cell. Other works from the

same authors reported bigger activities for the ORR on Pd-Ni catalysts compared with those obtained for Pd/C catalysts, with onset potential shifts of 100 mV towards positive values [70]. About other carbon supports different than carbon blacks, recently Calderon et al. supported Pd-Ni nanoparticles on previously chemically-treated carbon nanofibers [71]. The metal contents were close to 25 wt %, with 1:2 as Pd:Ni atomic ratio. The carbon nanofibers were enriched with surface oxygen and/or nitrogen groups after the chemical treatment. Although the onset potentials for ORR were more negative than that of the commercial catalyst Pd/C E-TEK, as well as this material displayed the highest diffusional current densities, higher mass activities i_k were determined for the Pd-Ni materials at 0.85 V, indicating the suitability of this alloy as possible replacement of Pt in DMFC cathodes. On the other hand, the catalyst supported on the carbon nanofibers with surface nitrogen groups displayed low production of hydrogen peroxide, suggesting an inhibiting effect of these functional groups toward the formation of this intermediate. The opposite behavior was observed for the catalysts supported on the O-modified carbon nanofibers (catalyst Pd-Ni/CNFO).

Similar to the case of platinum cathodes, cobalt has also been alloyed with palladium for cathode electrode applications in DMFCs. A recent work from Arroyo-Ramírez et al. [72] reported the use of organometallic complexes as precursors for synthesizing palladium-cobalt nanoparticles on Vulcan XC-72R carbon black, obtaining different ratios between Pd and Co (Pd_2Co/C and $PdCo_2/C$). A thermal reduction method was employed, which produced catalysts with high activity towards the ORR, even overcoming the performances of the commercial Pd/C catalyst. On the other hand, the tolerance to the methanol crossover of the synthesized materials was also higher than that of a Pt/C catalyst. The small particle diameters were obtained with the chemical reduction, being a crucial factor that conditioned the activity of the as-synthesized catalysts. Golmohammadi and co-workers proposed a novel alternative carbon support, consisting of the mixture between Vulcan XC-72R carbon black (VC) and multiwalled carbon nanotubes (MWCNTs), for supporting Pd_3Co nanoparticles [73]. The lowest potential drops and highest power densities were achieved with a MWCNTs/VC mass ratio close to 25:75. Presence of MWCNTs generated high surface area, major conductivity, and thus, fast ORR kinetics. Durability of membrane electrode assembly (MEA) with the mentioned mass ratio in the carbon support was also evaluated, finding both, high stability and improved durability, concluding that synergism between MWCNTs and VC contributed to the high performance of this catalyst.

Pd-Cu alloys are another promising alternative for carry out this reaction. Wu et al. [74] reported the wet chemical synthesis of Pd_nCu_{100-n} nanoalloys with controlled composition, finding that size, Pd/Cu ratio and phase structure of the nanoparticles are the key factors in the electrocatalytic activity and stability of these materials. The observed crystalline domains of the catalysts depended on the preparation method and influenced the performance of the catalysts, being the Pd_nCu_{100-n} catalysts with a Pd/Cu ratio close to 50:50, the most efficient toward the ORR, a fact explained from the body-centered cubic type ordered domains. The results from the structural and electrochemical characterizations suggested different correlations between the catalytic activity, atomic-scale structure and composition of the materials, bearing in mind the changes presented for $Pd_{50}Cu_{50}/C$ after the durability potential cycling. Other work reported the preparation of ternary catalyst with Pd, Cu and Co, increasing their activity and durability with the incorporation of gold traces [75] this noble metal galvanically replaced Co and Cu and entered into the Pd-Co-Cu lattice. The catalyst with the major durability (close to 100 h) was the $Au-Pd_6CoCu/C$, according with the results displayed by the single fuel-cell test, a result attributed to the homogeneous distribution of gold into the nanoparticles and the enhanced charge transfer between Pd and Au.

Fe is another metal with interesting properties in the catalysis of oxygen reduction. Neergat et al. investigated Pd-Fe alloys supported on carbon black, obtaining materials with high activity toward the ORR in comparison with the behavior observed for a Pd/C. Particularly, the Pd_3Fe/C catalyst displayed a half-wave potential more positive (>100 mV compared with that from Pd/C) and even similar than that of Pt/C with the same noble metal content [76]. Moreover, this catalyst showed both, a similar hydrogen peroxide production than that of Pt/C, but lower than that from Pd/C. The high

tolerance to the methanol poisoning was also observed, making it useful in an eventual methanol crossover condition. Another example of this alloy could be the study made by Abo-Zeid et al. [77], who synthesized Pd-Fe alloys by a combined ethylene glycol-sodium borohydride procedure in presence of PDDA ionic polycation. Some heat treatments at 300, 500 and 700 °C were applied to these catalysts, which exhibited a better performance in terms of activity and stability. In fact, the most important improvements were obtained with an aging temperature of 300 °C. The effects of heat treatment were associated with the increase of crystallite sizes and alloying degrees. Within the context of Pd-Fe alloys, Rivera and co-workers studied the activity of Pd, PdFe, PdIr and PdFeIr alloys toward the ORR [78]. Main results indicated that insertion of Fe and Ir in the Pd lattice enhanced the activity toward the ORR, as well as increased the methanol tolerance, depending of the redox state of the transition metals. For example, the RDE tests demonstrated that absence of Ir and presence of Fe^{2+} and Fe^{3+} and Ir^{3+} and Ir^{4+} coincide with a promoted activity in presence of methanol. This behavior was verified with the membrane electrode assembly tests performed for a cathode containing the PdFeIr/C catalyst, which yielded the highest performance. Thus, material surface structure has a high impact on the activity of catalysts, as well as the iridium introduction into the Pd alloy promoted the methanol tolerance and inhibited the water dissociation, diminishing the oxidation of catalyst surface.

Finally, we can cite a very recent work regarding an alloyed Pd-W catalysts and its performance toward the ORR [79]. This material showed a good dispersion of their nanoparticles on Vulcan XC-72R carbon black support, a fact that increased the electrochemical activity, as demonstrated from the electrochemical tests performed for $Pd_{19}W/C$, which displayed a two-fold superior mass activity in comparison with that of Pd/C This result postulated this catalyst as hopeful for cathode application in DMFCs. Table 6 summarizes the ORR onset potential values determined for some carbon-supported Pd-based catalysts.

Table 6. Onset potential values for the ORR performed on carbon-supported Pd-based catalysts.

Catalyst	Onset Potential (V vs. RHE)	Reference
Pd/AC	0.584	
Pd/CNF$_{fisbone}$	0.624	[63]
Pd/CNF$_{platelet}$	0.764	
Pd/MWCNTs	1.014	[64]
Pd/MWCNTs-Nafion composite	0.900	[67]
Pd/MWCNTs-PVP composite	0.870	
Pd$_{nanocubes}$/Vulcan XC-72R	1.000	[65]
Pd$_{nanoclusters}$/XC-72R (Ligand on)	0.897	
Pd$_{nanoclusters}$/XC-72R (Ligand off)	1.017	[66]
Pt/XC-72R	0.987	
Pd/C	1.085	
Pd-Ni(3:1)/C	1.085	[68]
Pd-Ni(1:1)/C	1.105	
Pd-Ni(1:3)/C	1.005	
Pd/C E-TEK	1.050	
Pd-Ni/CB 1:2	0.960	
Pd-Ni/CNF 1:2	0.955	[71]
Pd-Ni/CNFO 1:2	0.960	
Pd-Ni/CNFN 1:2	0.940	
Pd/C (commercial)	0.728	
Pd$_2$Co/C	0.735	
PdCo$_2$/C	0.731	[72]
PtCo/C (commercial)	0.836	
Pt/C (commercial)	0.844	
Pd-Cu(36:64)/C	0.799	
Pd-Cu(54:46)/C	0.919	
Pd-Cu(75:25)/C	0.799	[74]
Pd/C (commercial)	0.879	

Table 6. *Cont.*

Catalyst	Onset Potential (V vs. RHE)	Reference
Pd-Fe/C (non-heat treated)	0.655	
Pd-Fe/C (300 °C)	0.865	[77]
Pd-Fe/C (500 °C)	0.815	
Pd-Fe/C (700 °C)	0.805	
Pd/C	0.940	
$Pd_{19}W/C$	0.950	
Pd_9W/C	0.950	[79]
Pd_3W/C	0.950	
JM Pt/C	0.950	

From the data presented in the Table 6, it is possible to conclude that the more active palladium catalysts toward the ORR are those alloyed with nickel, bearing in mind they showed the more positive onset potentials for this reaction [68]. The metal content of these materials was close to 12 wt %, suggesting that a small content of Pd is enough for achieving a good performance. The most positive onset potential was presented by the catalyst Pd-Ni (1:1)/C, demonstrating that composition is a determining factor to produce high ORR current densities with the most positive onset potential. Moreover, alloys between palladium and tungsten also presented positive onset potentials (values close to 0.95 V vs. RHE) [79], especially in the case of the catalyst $Pd_{19}W/C$. Only a few amount of tungsten alloyed with palladium was enough to obtain a remarkable increase in the catalytic activity in comparison with the results displayed for the Pd/C catalyst. Therefore, Ni and W are suitable metals to be alloyed with palladium to be used as cathodes for DMFCs.

3.2. Non Carbon-Supported Pd-Alloys

Pd catalysts supported on non-carbonaceous materials for the ORR have also been investigated, reaching an increased interest because of the possibilities for obtaining materials with novel properties and synergistic effects between metal nanoparticles and support, enabling the activity and the performance of cathodes in DMFCs. One alternative could be the doping of perovskites with Pd atoms at different oxidation states, as exposed by Zhu et al. [80], who reported that incorporation of the rare $Pd^{3/4+}$ oxidation state favorably affects the catalytic activity of perovskites. This fact resulted in the obtaining of a mass activity 2.5—higher than that of a Pt/C commercial catalyst. Moreover, this material displayed better durability and tolerance to methanol crossover. The authors suggested that this increase can be attributed to the reduction in the atomic distances between the atoms conforming the perovskite and the modifying of the d-band center, generating a decrease in the electron density, a weak linking between Pd and OH_{ads} and the availability of more active sites.

In the previous section, we mentioned some works related with the use of TiO_2 as support in Pd-alloyed anode catalysts. Some reports indicate that TiO_2 could be also employed as support for cathode catalysts. Lo Vecchio and co-workers [81] reported the preparation of Pd catalysts supported on titanium sub-oxides with formula Pd/Ti_nO_{2n-1}. This support conferred to the catalyst high stability and resistance after 1000 potential cycles, as well as better tolerance to the methanol poisoning, as corroborated by means of the onset potential shifts, which were displaced toward negative values for the Pt/C catalyst in presence of methanol, whereas in the case of the Pd/Ti_nO_{2n-1} this potential was constant.

Tungsten and molybdenum have also been employed for design supports. Ko et al. [82] synthesized mesoporous tungsten carbide in order to test them as catalysts and also as support for Pd nanoparticles. The materials were built in a CH_4/H_2 atmosphere using tungsten nitride nanoparticles as starting material, varying the temperatures (700, 800 and 900 °C). The authors detected a correlation between the pore structures and the reaction temperature, considering that 900 °C was the temperature that produced the tungsten carbide with the best electrocatalytic properties (most positive onset potentials, highest oxygen reduction current densities and lowest production of hydrogen peroxide).

When the Pd nanoparticles were supported on these materials, the new catalysts displayed high durability and stability after 2000 cycles. In fact, the corrosion resistance was higher than that of a Pt/C catalyst with the same metal contents. In the case of molybdenum, Yan and co-workers [83] synthesized bimetallic carbide Fe_2MoC for anchoring Pd nanoparticles with high activity and stability compared to a Pd/C and a commercial Pt/C in the ORR. The authors attributed the remarkable performance of Pd/GC-Fe_2MoC to an electron-donating effect from the Fe_2MoC to the supported Pd nanoparticles, which promoted the linkage strength between them. The Koutecky-Levich analysis of this material suggested water as major product during the ORR, after finding a four-electron transfer. In other kind of composites, Zuo et al. [84] prepared MoS_2/Pd catalysts by a sonochemical method. This method consisted of the ultrasonic exfoliation of bulk MoS_2 into single and few layers nanosheets, which then were employed as support for Pd nanoparticles. Electrochemical measurements made by cyclic voltammetry and rotating disk electrode showed a direct four-electron pathway for the ORR, with high electrocatalytic activity and long operation stability than a commercial Pt/C catalyst. In fact, mass and specific activities of this composite overcame that from the commercial catalyst. Catalysts containing Ti also have been synthesized from dealloying processes, displaying good results in the ORR. Chen and co-workers [85] applied this method for developing a nanoporous PdCuTiAl (np-PdCuTiAl) electrocatalyst with a three-dimensional network conformed by ultrafine channels. This composite displayed a half-wave potential more positive than those exhibited by Pd/C and Pt/C catalysts, with a four-electron reaction pathway. Moreover, the tolerance toward the methanol poisoning was major than that observed for the carbon supported-Pd and Pt catalysts.

Unsupported Pd-Ni alloyed catalysts have also been prepared and tested towards ORR. Xu et al. [86] dealloyed a PdNiAl precursor alloy to make a rich-nanoporous PdNi alloy. The as-synthesized electrode displayed a uniform structure with an interconnected network of hollow channels with a 5 nm-diameter approximately. The electrochemical tests for this material demonstrated a high activity towards the ORR, in terms of the bigger specific and mass activities in comparison with a commercial Pt/C, besides a longer durability and tolerance to methanol. The characteristics of the three-dimensional network and the synergistic effect between Ni and Pd were stated by the authors as key factors for the improved performance of this material. Dealloying process was also employed by Chen et al. [87], who fabricated a nanoporous PdNi catalyst by electrochemical dealloying. The starting material was a $Pd_{20}Ni_{80}$ alloy, which was putted in an acid solution to be dealloyed, obtaining a final Ni content of 9 at %. This material displayed higher electrocatalytic performances during the oxygen reduction than both, a commercial Pd/C and nanoporous Pd catalysts, with more positive onset potentials and enhanced mass activities. As mentioned above, the remarkable behavior of this alloy was attributed to the bimetallic synergistic effect and the well-connected porosity of the material. Within the line of the non-supported materials, Xiong and co-workers [88] synthesized a self-supported Pd-Cu catalyst with 3D porous structure, using an electrochemical deposition of copper from a $CuSO_4$ solution in acid media, in order to promote a galvanic replacement with the Pd^{2+} present in a Na_2PdCl_4 solution. The most important properties of the electrochemically synthesized catalyst were related with its long-term stability and the high oxygen reduction current densities, overcoming those of a Pt/C catalyst. The onset potentials on these materials were close to 1.0 V vs. RHE, while Pt/C exhibited a value closer to 0.9 V. Table 7 shows some of the parameters observed during the ORR on non-carbon supported catalysts.

The onset potential differences between the commercial catalysts and those tested during the ORR indicated that the alloying process of PdNi catalysts is a promising technique to obtain cathodes for fuel cells. Xu et al. [86] demonstrated that it is possible to dealloy PdNiAl composites to obtain PdNi structures with similar activity to a Pt/C commercial catalyst, this fact representing a decrease in the overall production costs of DMFCs. The three dimensional nanostructure and the changes induced by Ni in the electronic structure of palladium seems to be the factors influencing the outstanding performance of these materials.

Table 7. Onset potential values for the ORR performed on non-carbon-supported Pd-based catalysts.

Catalyst	Onset Potential (V vs. RHE)	Reference
Pd/LF	0.662	
Pd/LFP0.05	0.792	[80]
Pd/LFP0.05-R	0.722	
Pd/LFP0.05-RO	0.772	
Pd/WC-700-m	0.692	
Pd/WC-800-m	0.812	[82]
Pd/WC-900-m	0.872	
Pt/C	1.08	
Pd/C	0.92	[83]
Pd/C-MoC	0.95	
Pd/C-Fe$_2$MoC	1.08	
Pt/C (commercial)	1.04	
PdNi dealloyed	1.04	[86]
Pd dealloyed	0.90	
Pt/C (commercial)	0.90	[88]
Pd-Cu(nanodendrites)	1.00	

4. Conclusions

In this review, a revision about the state of the art of Pd-based catalysts has been described, in terms of the efficiency and performance towards both the methanol oxidation and oxygen reduction reactions, as fundamental chemical processes in direct methanol fuel cells (DMFCs). The most important conclusion in the case of the catalysts suggested as anodes for DMFCs is related with the role of second metal in the forming of OH$_{ads}$, bearing in mind its importance in the oxidizing of CO and others intermediates generated during the oxidation of methanol. Different authors have reported that these metals (Ag, Ni, and Rh) are able to form OH$_{ads}$ at lower potentials than those determined for Pd or Pt, whereas novel carbon materials increase the diffusion of electroactive species and facilitate the electronic transference. On the other hand, novel non-carbon materials as supports create synergistic effects that improve the performance of anodes, basically by means of some changes in the electronic structure of catalytic metals, favoring the oxidation of methanol and the other species related with this reaction. In the case of the cathode Pd-based catalysts, the decrease of the onset potentials and the enhance current densities detected during the ORR were the most important parameters considered to assess the performance of the catalysts. In this sense, the low content of surface Pd oxides and the structure of support were started as crucial factors to obtain good values for the mentioned parameters. Crystalline structure also seems to promote the formation of more active sites and upgrade the tolerance of methanol towards the methanol crossover. Pd-Ni and Pd-W seems to be the most promising cathode catalysts, bearing in mind their positive onset potentials (some of them, overcoming those observed for commercial Pd and Pt catalysts), indicating the beneficial effects of the second metal incorporation on the structure of palladium. From the works here cited and revised, it is possible to conclude that replacement of platinum in the electrodes for direct methanol fuel cells could be carried out, using Pd and Pd-alloys catalysts supported on both, carbon materials and non-carbon materials, in order to decrease the consumption of this metal as catalytic phase in direct methanol fuel cells.

Author Contributions: Juan Carlos Calderón Gómez wrote the paper; Rafael Moliner and Maria Jesus Lázaro revised the paper.

Conflicts of Interest: The authors declare no conflict of interest.

Abbreviations

The following abbreviations are used in this manuscript:

DMFC   Direct Methanol Fuel Cells
CNT   Carbon Nanotubes
MWCNT   Multi-Walled Carbon Nanotubes
RGO   Reduced Graphene Oxide (by sodium borohydride)
MOR   Methanol oxidation reaction
MEA   Membrane electrode assembly
DEMS   Differential Electrochemical Mass Spectrometry
ORR   Oxygen Reduction Reaction
VC   Vulcan Carbon
TKK   Tanaka Kikinzoku Kogyo®

References

1. Lee, J.B.; Park, Y.K.; Yang, O.B.; Kang, Y.K.; Jun, K.W.; Lee, Y.J.; Kim, H.Y.; Lee, K.H.; Choi, W.C. Synthesis of porous carbons having surface functional groups and their application to direct-methanol fuel cells. *J. Power Sources* **2006**, *158*, 1251–1255. [CrossRef]

2. Brouzgou, A.; Song, S.Q.; Tsiakaras, P. Low and non-platinum electrocatalysts for PEMFCs: Current status, challenges and prospects. *Appl. Catal. B* **2012**, *127*, 371–388. [CrossRef]

3. Fournier, J.; Faubert, G.; Tilquin, J.Y.; Cote, R.; Guay, D.; Dodelet, J.P. High-performance, low Pt content, catalysts for the electroreduction of oxygen in polymer electrolyte fuel cells. *J. Electrochem. Soc.* **1997**, *144*, 145–154. [CrossRef]

4. Lefèvre, M.; Dodelet, J.P.; Bertrand, P. Molecular oxygen reduction in PEM fuel cells: Evidence for the simultaneous presence of two active sites in Fe-based catalysts. *J. Phys. Chem. B* **2002**, *106*, 8705–8713. [CrossRef]

5. Matter, P.H.; Zhang, L.; Ozkan, U.S. The role of nanostructure in nitrogen-containing carbon catalysts for the oxygen reduction reaction. *J. Catal.* **2006**, *239*, 83–96. [CrossRef]

6. Zaikovskii, V.I.; Nagabhushana, K.S.; Kriventsov, V.V.; Loponov, K.N.; Cherepanova, S.V.; Kvon, R.I.; Bönnemann, H.; Kochubey, D.I.; Savinova, E.R. Synthesis and structural characterization of Se-modified carbon-supported Ru nanoparticles for the oxygen reduction reaction. *J. Phys. Chem. B* **2006**, *110*, 6881–6890. [CrossRef] [PubMed]

7. Serov, A.A.; Min, M.; Chai, G.; Han, S.; Kang, S.; Kwak, C. Preparation, characterization, and high performance of RuSe/C for direct methanol fuel cells. *J. Power Sources* **2008**, *175*, 175–182. [CrossRef]

8. Mustain, W.E.; Prakash, J. Kinetics and mechanism for the oxygen reduction reaction on polycrystalline cobalt-palladium electrocatalysts in acid media. *J. Power Sources* **2007**, *170*, 28–37. [CrossRef]

9. Assiongbon, K.A.; Roy, D. Electro-oxidation of methanol on gold in alkaline media: Adsorption characteristics of reaction intermediates studied using time resolved electro-chemical impedance and surface plasmon resonance techniques. *Surf. Sci.* **2005**, *594*, 99–119. [CrossRef]

10. Hu, F.P.; Shen, P.K. Ethanol oxidation on hexagonal tungsten carbide single nanocrystal-supported Pd electrocatalyst. *J. Power Sources* **2007**, *173*, 877–881. [CrossRef]

11. Li, R.S.; Wei, Z.; Huang, T.; Yu, A.S. Ultrasonic-assisted synthesis of Pd–Ni alloy catalysts supported on multi-walled carbon nanotubes for formic acid electrooxidation. *Electrochimica Acta* **2011**, *56*, 6860–6865. [CrossRef]

12. Shao, M.H. Palladium-based electrocatalysts for hydrogen oxidation and oxygen reduction reactions. *J. Power Sources* **2011**, *196*, 2433–2444. [CrossRef]

13. Nguyen, S.T.; Tan, D.S.L.; Lee, J.M.; Chan, S.H.; Wang, J.Y.; Wang, X. Tb promoted Pd/C catalysts for the electrooxidation of ethanol in alkaline media. *Int. J. Hydrogen Energy* **2011**, *36*, 9645–9652. [CrossRef]

14. Grden, M.; Łukaszewski, M.; Jerkiewicz, G.; Czerwinski, A. Electrochemical behavior of palladium electrode: Oxidation, electrodissolution and ionic adsorption. *Electrochimica Acta* **2008**, *53*, 7583–7598. [CrossRef]

15. Bianchini, C.; Shen, P.K. Palladium-based electrocatalysts for alcohol oxidation in half cells and in direct alcohol fuel cells. *Chem. Rev.* **2009**, *109*, 4183–4206. [CrossRef] [PubMed]

16. Wei, Y.C.; Liu, C.W.; Wang, K.W. Improvement of oxygen reduction reaction and methanol tolerance characteristics for PdCo electrocatalysts by Au alloying and CO treatment. *Chem. Commun.* **2011**, *47*, 11927–11929. [CrossRef] [PubMed]

17. Calderón, J.C.; Mahata, N.; Pereira, M.F.R.; Figueiredo, J.L.; Fernandes, V.R.; Rangel, C.M.; Calvillo, L.; Lazaro, M.J.; Pastor, E. Pt–Ru catalysts supported on carbon xerogels for PEM fuel cells. *Int. J. Hydrogen Energy* **2012**, *37*, 7200–7211.

18. Yu, X.W.; Ye, S.Y. Recent advances in activity and durability enhancement of Pt/C catalytic cathode in PEMFC: Part I. Physico-chemical and electronic interaction between Pt and carbon support, and activity enhancement of Pt/C catalyst. *J. Power Sources* **2007**, *172*, 133–144. [CrossRef]

19. Zhang, W.Y.; Yao, Q.S.; Wu, X.D.; Fu, Y.S.; Deng, K.M.; Wang, X. Intimately coupled hybrid of graphitic carbon nitride nanoflakelets with reduced graphene oxide for supporting Pd nanoparticles: A stable nanocatalyst with high catalytic activity towards formic acid and methanol electrooxidation. *Electrochim Acta* **2016**, *200*, 131–141. [CrossRef]

20. Zhang, X.; Zhu, J.X.; Tiwary, C.S.; Ma, Z.Y.; Huang, H.J.; Zhang, J.F.; Lu, Z.Y.; Huang, W.; Wu, Y.P. Palladium nanoparticles supported on nitrogen and sulfur dual-doped graphene as highly active electrocatalysts for formic acid and methanol oxidation. *ACS Appl. Mater. Interfaces* **2016**, *8*, 10858–10865. [CrossRef] [PubMed]

21. Zhang, W.Y.; Huang, H.J.; Li, F.; Deng, K.M.; Wang, X. Palladium nanoparticles supported on graphitic carbon nitride-modified reduced graphene oxide as highly efficient catalysts for formic acid and methanol electrooxidation. *J. Mat. Chem. A* **2014**, *2*, 19084–19094. [CrossRef]

22. Yin, Z.; Zhang, Y.N.; Chen, K.; Li, J.; Li, W.J.; Tang, P.; Zhao, H.B.; Zhu, Q.J.; Bao, X.H.; Ma, D. Monodispersed bimetallic PdAg nanoparticles with twinned structures: Formation and enhancement for the methanol oxidation. *Sci. Rep.* **2014**, *4*, 4288–4296. [CrossRef] [PubMed]

23. Wang, Y.; Sheng, Z.M.; Yang, H.B.; Jiang, S.P.; Li, C.M. Electrocatalysis of carbon black- or activated carbon nanotubes-supported Pd–Ag towards methanol oxidation in alkaline media. *Int. J. Hydrogen Energy* **2010**, *35*, 10087–10093. [CrossRef]

24. Luo, B.; Liu, S.M.; Zhi, L.J. Chemical approaches toward graphene-based nanomaterials and their applications in energy-related areas. *Small* **2012**, *8*, 630–646. [CrossRef] [PubMed]

25. Li, L.Z.; Chen, M.X.; Huang, G.B.; Yang, N.; Zhang, L.; Wang, H.; Liu, Y.; Wang, W.; Gao, J.P. A green method to prepare Pd–Ag nanoparticles supported on reduced graphene oxide and their electrochemical catalysis of methanol and ethanol oxidation. *J. Power Sources* **2014**, *263*, 13–21. [CrossRef]

26. Jurzinsky, T.; Cremers, C.; Pinkwart, K.; Tübke, J. On the influence of Ag on Pd-based electrocatalyst for methanol oxidation in alkaline media: A comparative differential electrochemical mass spectrometry study. *Electrochimica Acta* **2016**, *199*, 270–279. [CrossRef]

27. Shen, P.K.; Xu, C.W.; Zeng, R.; Liu, Y.L. Electro-oxidation of methanol on NiO-promoted Pt/C and Pd/C catalysts. *Electrochem. Solid-State Lett.* **2006**, *9*, A39–A42. [CrossRef]

28. Li, G.L.; Jiang, L.H.; Jiang, Q.; Wang, S.L.; Sun, G.Q. Preparation and characterization of Pd_xAg_y/C electrocatalysts for ethanol electrooxidation reaction in alkaline media. *Electrochimica Acta* **2011**, *56*, 7703–7711. [CrossRef]

29. Qi, Z.; Geng, H.; Wang, X.; Zhao, C.; Ji, H.; Zhang, C.; Xu, J.; Zhang, Z. Novel nanocrystalline PdNi alloy catalysts for methanol and ethanol electro-oxidation in alkaline media. *J. Power Sources* **2011**, *196*, 5823–5828. [CrossRef]

30. Amin, R.S.; Abdel Hameed, R.M.; El-Khatiba, K.M. Microwave heated synthesis of carbon supported Pd, Ni and Pd–Ni nanoparticles for methanol oxidation in KOH solution. *Appl. Catal. B* **2014**, *148-149*, 557–567. [CrossRef]

31. Amin, R.S.; Abdel Hameed, R.M.; El-Khatib, K.M.; Elsayed Youssef, M. Electrocatalytic activity of nanostructured Ni and Pd–Ni on Vulcan XC-72R carbon black for methanol oxidation in alkaline medium. *Int. J. Hydrogen Energy* **2014**, *39*, 2026–2041. [CrossRef]

32. Liu, Z.L.; Zhang, X.H.; Hong, L. Physical and electrochemical characterization of nanostructured Pd/C and PdNi/C catalysts for methanol oxidation. *Electrochem. Commun.* **2009**, *11*, 925–928. [CrossRef]

33. Calderón, J.C.; Nieto-Monge, M.J.; Pérez-Rodríguez, S.; Pardo, J.I.; Moliner, R.; Lázaro, M.J. Palladium–nickel catalysts supported on different chemically-treated carbon blacks for methanol oxidation in alkaline media. *Int. J. Hydrogen Energy* **2016**. [CrossRef]

34. Singh, R.N.; Singh, A.; Anindita. Electrocatalytic activity of binary and ternary composite films of Pd, MWCNT and Ni, Part II: Methanol electrooxidation in 1 M KOH. *Int. J. Hydrogen Energy* **2009**, *34*, 2052–2057. [CrossRef]

35. Zhao, Y.C.; Zhan, L.; Tian, J.N.; Nie, S.L.; Ning, Z. MnO$_2$ modified multi-walled carbon nanotubes supported Pd nanoparticles for methanol electro-oxidation in alkaline media. *Int. J. Hydrogen Energy* **2010**, *35*, 10522–10526. [CrossRef]

36. Sasahara, A.; Tamura, H.; Tanaka, K.I. Catalytic activity of Pt-deposited Rh(110) bimetallic surface for NO + H$_2$ reaction. *J. Phys. Chem. B* **1997**, *101*, 1186–1189. [CrossRef]

37. Ross, P.N.; Kinoshita, K.; Scarpellino, A.J.; Stonehart, P. Electrocatalysis on binary alloys: I. Oxidation of molecular hydrogen on supported Pt−Rh alloys. *J. Electroanal. Chem. Interfacial Electrochem.* **1975**, *59*, 177–189. [CrossRef]

38. Shen, S.Y.; Zhao, T.S.; Xu, J.B. Carbon supported PtRh catalysts for ethanol oxidation in alkaline direct ethanol fuel cell. *Int. J. Hydrogen Energy* **2010**, *35*, 12911–12917. [CrossRef]

39. de Souza, J.P.I.; Queiroz, S.L.; Bergamaski, K.; Gonzalez, E.R.; Nart, F.C. Electro-oxidation of ethanol on Pt, Rh, and PtRh electrodes. A study using DEMS and in-situ FTIR techniques. *J. Phys. Chem. B* **2002**, *106*, 9825–9830. [CrossRef]

40. Bergamaski, K.; Gonzalez, E.R.; Nart, F.C. Ethanol oxidation on carbon supported platinum-rhodium bimetallic catalysts. *Electrochimica Acta* **2008**, *53*, 4396–4406. [CrossRef]

41. Delpeuch, A.B.; Asset, T.; Chatenet, M.; Cremers, C. Electrooxidation of ethanol at room temperature on carbon-supported Pt and Rh-containing catalysts: A DEMS study. *J. Electrochem. Soc.* **2014**, *161*, F918–F924. [CrossRef]

42. Jurzinsky, T.; Bär, R.; Cremers, C.; Tübke, J.; Elsner, P. Highly active carbon supported palladium-rhodium Pd$_x$Rh/C catalysts for methanol electrooxidation in alkaline media and their performance in anion exchange direct methanol fuel cells (AEM-DMFCs). *Electrochimica Acta* **2015**, *176*, 1191–1201. [CrossRef]

43. Hsieh, C.T.; Yu, P.Y.; Tzou, D.Y.; Hsu, J.P.; Chiu, Y.R. Bimetallic Pd–Rh nanoparticles onto reduced graphene oxide nanosheets as electrocatalysts for methanol oxidation. *J. Electroanal. Chem.* **2016**, *761*, 28–36. [CrossRef]

44. Alvi, M.A.; Akhtar, M.S. An effective and low cost Pd–Ce bimetallic decorated carbon nanofibers as electrocatalyst for direct methanol fuel cells applications. *J. Alloys Compd.* **2016**, *684*, 524–529. [CrossRef]

45. He, L.L.; Song, P.; Feng, J.J.; Fang, R.; Yu, D.X.; Chen, J.R.; Wang, A.J. Porous dandelion-like gold@ palladium core-shell nanocrystals in-situ growth on reduced graphene oxide with improved electrocatalytic properties. *Electrochimica Acta* **2016**, *200*, 204–213. [CrossRef]

46. Zhang, S.S.; Yuan, X.Z.; Wang, H.J.; Mérida, W.; Zhu, H.; Shen, J.; Wu, S.H.; Zhang, J.J. A review of accelerated stress tests of MEA durability in PEM fuel cells. *Int. J. Hydrogen Energy* **2009**, *34*, 388–404. [CrossRef]

47. Niu, X.H.; Zhao, H.L.; Lan, M.B. Palladium deposits spontaneously grown on nickel foam for electrocatalyzing methanol oxidation: Effect of precursors. *J. Power Sources* **2016**, *306*, 361–368. [CrossRef]

48. Park, K.W.; Han, S.B.; Lee, J.M. Photo (UV)-enhanced performance of Pt–TiO$_2$ nanostructure electrode for methanol oxidation. *Electrochem. Commun.* **2007**, *9*, 1578–1581. [CrossRef]

49. Xue, X.D.; Gu, L.; Cao, X.B.; Song, Y.Y.; Zhu, L.W.; Chen, P. One-pot, high-yield synthesis of titanate nanotube bundles decorated by Pd (Au) clusters for stable electrooxidation of methanol. *J. Solid State Chem.* **2009**, *182*, 2912–2917. [CrossRef]

50. Guo, X.; Guo, D.J.; Qiu, X.P.; Chen, L.Q.; Zhu, W.T. Excellent dispersion and electrocatalytic properties of Pt nanoparticles supported on novel porous anatase TiO$_2$ nanorods. *J. Power Sources* **2009**, *194*, 281–285. [CrossRef]

51. Dvoranova, D.; Brezova, V.; Mazur, M.; Malati, M.A. Investigations of metal-doped titanium dioxide photocatalysts. *Appl. Catal. B* **2002**, *37*, 91–105. [CrossRef]

52. Wang, M.; Guo, D.J.; Li, H.L. High activity of novel Pd/TiO$_2$ nanotube catalysts for methanol electro-oxidation. *J. Solid State Chem.* **2005**, *178*, 1996–2000. [CrossRef]

53. Hosseini, M.G.; Momeni, M.M.; Khalilpur, H. Synthesis and characterization of palladium nanoparticles immobilized on TiO$_2$ nanotubes as a new high active electrode for methanol electro-oxidation. *Int. J. Nanosci.* **2012**, *11*, 1250016. [CrossRef]

54. Ju, J.; Shi, Y.; Wu, D. TiO$_2$ nanotube supported PdNi catalyst for methanol electro-oxidation. *Powder Technol.* **2012**, *230*, 252–256. [CrossRef]

55. Cao, S.; Xu, W.; Zhu, S.; Liang, Y.; Li, Z.; Cui, Z.; Yang, X.; Inoue, A. Synthesis of TiO_2 nanoparticles loaded Pd/CuO nanoporous catalysts and their catalytic performance for methanol, ethanol and formic acid electro-oxidations. *J. Electrochem. Soc.* **2016**, *163*, E263–E271. [CrossRef]

56. Fernandez, J.L.; Walsh, D.A.; Bard, A.J. Thermodynamic guidelines for the design of bimetallic catalysts for oxygen electroreduction and rapid screening by scanning electrochemical microscopy. M–Co (M: Pd, Ag, Au). *J. Am. Chem. Soc.* **2005**, *127*, 357–365. [CrossRef] [PubMed]

57. Shukla, A.K.; Raman, R.K. Methanol-resistant oxygen-reduction catalysts for direct methanol fuel cells. *Annu. Rev. Mater. Res.* **2003**, *33*, 155–168. [CrossRef]

58. Baranton, S.; Coutanceau, C.; Roux, C.; Hahn, F.; Leger, J.M. Oxygen reduction reaction in acid medium at iron phthalocyanine dispersed on high surface area carbon substrate: tolerance to methanol, stability and kinetics. *J. Electroanal. Chem.* **2005**, *577*, 223–234. [CrossRef]

59. Wagner, A.J.; Wolfe, G.M.; Fairbrother, D.H. Reactivity of vapor-deposited metal atoms with nitrogen-containing polymers and organic surfaces studied by in situ XPS. *Appl. Surf. Sci.* **2003**, *219*, 317–328. [CrossRef]

60. Matter, P.H.; Zhang, L.; Ozkan, U.S. The role of nanostructure in nitrogen-containing carbon catalysts for the oxygen reduction reaction. *J. Catal.* **2006**, *239*, 83–96. [CrossRef]

61. Mustain, W.E.; Kepler, K.; Prakash, J. Investigations of carbon-supported $CoPd_3$ catalysts as oxygen cathodes in PEM fuel cells. *Electrochem. Commun.* **2006**, *8*, 406–410. [CrossRef]

62. Serov, A.A.; Cho, S.Y.; Han, S.; Min, M.; Chai, G.; Nam, K.H.; Kwak, C. Modification of palladium-based catalysts by chalcogenes for direct methanol fuel cells. *Electrochem. Commun.* **2007**, *9*, 2041–2044. [CrossRef]

63. Zheng, J.S.; Zhang, X.; Li, P.; Zhu, J.; Zhou, X.G.; Yuan, W.K. Effect of carbon nanofiber microstructure on oxygen reduction activity of supported palladium electrocatalyst. *Electrochem. Commun.* **2007**, *9*, 895–900. [CrossRef]

64. Chakraborty, S.; Retna Raj, C. Electrocatalytic performance of carbon nanotube-supported palladium particles in the oxidation of formic acid and the reduction of oxygen. *Carbon* **2010**, *48*, 3242–3249. [CrossRef]

65. Lüsi, M.; Erikson, H.; Sarapuu, A.; Tammeveski, K.; Solla-Gullón, J.; Feliu, J.M. Oxygen reduction reaction on carbon-supported palladium nanocubes in alkaline media. *Electrochem. Commun.* **2016**, *64*, 9–13. [CrossRef]

66. Zhao, S.; Zhang, H.; House, S.D.; Jin, R.; Yang, J.C.; Jin, R. Ultrasmall palladium nanoclusters as effective catalyst for oxygen reduction reaction. *ChemElectroChem.* **2016**, *3*, 1225. [CrossRef]

67. Jukk, K.; Alexeyeva, N.; Johans, C.; Kontturi, K.; Tammeveski, K. Oxygen reduction on Pd nanoparticle/multi-walled carbon nanotube composites. *J. Electroanal. Chem.* **2012**, *666*, 67–75. [CrossRef]

68. Li, B.; Prakash, J. Oxygen reduction reaction on carbon supported palladium-nickel alloys in alkaline media. *Electrochem. Commun.* **2009**, *11*, 1162–1165. [CrossRef]

69. Ramos-Sanchez, G.; Santana-Salinas, A.; Vazquez-Huerta, G.; Solorza-Feria, O. Electrochemical impedance study and performance of PdNi nanoparticles as cathode catalyst in a polymer electrolyte membrane fuel cell. *J. New Mat. Electrochem. Syst.* **2010**, *13*, 213–217.

70. Ramos-Sánchez, G.; Yee-Madeira, H.; Solorza-Feria, O. PdNi electrocatalyst for oxygen reduction in acid media. *Int. J. Hydrogen Energy* **2008**, *33*, 3596–3600. [CrossRef]

71. Calderón, J.C.; Celorrio, V.; Nieto-Monge, M.J.; Fermín, D.J.; Pardo, J.I.; Moliner, R.; Lázaro, M.J. Palladium-nickel materials as cathode electrocatalysts for alkaline fuel cells. *Int. J. Hydrogen Energy* **2016**. accepted for publication.

72. Arroyo-Ramírez, L.; Montano-Serrano, R.; Luna-Pineda, T.; Román, F.R.; Raptis, R.G.; Cabrera, C.R. Synthesis and characterization of palladium and palladium-cobalt nanoparticles on Vulcan XC-72R for the oxygen reduction reaction. *ACS Appl. Mater. Interfaces* **2013**, *5*, 11603–11612. [CrossRef] [PubMed]

73. Golmohammadi, F.; Gharibi, H.; Sadeghi, S. Synthesis and electrochemical characterization of binary carbon supported Pd_3Co nanocatalyst for oxygen reduction reaction in direct methanol fuel cells. *Int. J. Hydrogen Energy* **2016**, *41*, 7373–7387. [CrossRef]

74. Wu, J.; Shan, S.; Luo, J.; Joseph, P.; Petkov, V.; Zhong, C.J. PdCu nanoalloy electrocatalysts in oxygen reduction reaction: role of composition and phase state in catalytic synergy. *ACS Appl. Mater. Interfaces* **2015**, *7*, 25906–25913. [CrossRef] [PubMed]

75. Wang, D.; Liu, S.; Wang, J.; Lin, R.; Kawasaki, M.; Rus, E.; Silberstein, K.E.; Lowe, M.A.; Lin, F.; Nordlund, D.; et al. Spontaneous incorporation of gold in palladium-based ternary nanoparticles makes durable electrocatalysts for oxygen reduction reaction. *Nat. Commun.* **2016**. [CrossRef] [PubMed]

76. Neergat, M.; Gunasekar, V.; Rahul, R. Carbon-supported Pd–Fe electrocatalysts for oxygen reduction reaction (ORR) and their methanol tolerance. *J. Electroanal. Chem.* **2011**, *658*, 25–32. [CrossRef]

77. Abo Zeid, E.F.; Kim, Y.T. Effect of heat treatment on nanoparticle size and oxygen reduction reaction activity for carbon-supported Pd–Fe alloy electrocatalysts. *Am. J. Nano. Res. Appl.* **2015**, *3*, 71–77.

78. Rivera Gavidia, L.M.; García, G.; Anaya, D.; Querejeta, A.; Alcaide, F.; Pastor, E. Carbon-supported Pt-free catalysts with high specificity and activity toward the oxygen reduction reaction in acidic medium. *Appl. Catal. B* **2016**, *184*, 12–19. [CrossRef]

79. Dai, Y.; Yu, P.; Huang, Q.; Sun, K. Pd-W alloy electrocatalysts and their catalytic property for oxygen reduction. *Fuel Cells* **2016**, *16*, 165–169. [CrossRef]

80. Zhu, Y.; Zhou, W.; Chen, Y.; Yu, J.; Xu, X.; Su, C.; Tadé, M.O.; Shao, Z. Boosting oxygen reduction reaction activity of palladium by stabilizing Its unusual oxidation states in perovskite. *Chem. Mater.* **2015**, *27*, 3048–3054. [CrossRef]

81. Lo Vecchio, C.; Alegre, C.; Sebastián, D.; Stassi, A.; Aricò, A.S.; Baglio, V. Investigation of supported Pd-based electrocatalysts for the oxygen reduction reaction: performance, durability and methanol tolerance. *Materials* **2015**, *8*, 7997–8008. [CrossRef]

82. Ko, A.R.; Lee, Y.W.; Moon, J.S.; Han, S.B.; Cao, G.Z.; Park, K.W. Ordered mesoporous tungsten carbide nanoplates as non-Pt catalysts for oxygen reduction reaction. *Appl. Catal. A* **2014**, *477*, 102–108. [CrossRef]

83. Yan, Z.; Zhang, M.; Xie, J.; Zhu, J.; Shen, P.K. A bimetallic carbide Fe_2MoC promoted Pd electrocatalyst with performance superior to Pt/C towards the oxygen reduction reaction in acidic media. *Appl. Catal. B* **2015**, *165*, 636–641. [CrossRef]

84. Zuo, L.X.; Jiang, L.P.; Zhu, J.J. A facile sonochemical route for the synthesis of MoS_2/Pd composites for highly efficient oxygen reduction reaction. *Ultrason. Sonochem.* **2016**. [CrossRef] [PubMed]

85. Chen, X.; Si, C.; Wang, Y.; Ding, Y.; Zhang, Z. Multicomponent platinum-free nanoporous Pd-based alloy as an active and methanol-tolerant electrocatalyst for the oxygen reduction reaction. *Nano Res.* **2016**, *9*, 1831–1843. [CrossRef]

86. Xu, C.; Liu, Y.; Hao, Q.; Duan, H. Nanoporous PdNi alloys as highly active and methanol tolerant electrocatalysts towards oxygen reduction reaction. *J. Mater. Chem. A* **2013**, *1*, 13542–13548. [CrossRef]

87. Chen, L.; Guo, H.; Fujita, T.; Hirata, A.; Zhang, W.; Inoue, A.; Chen, M. Nanoporous PdNi bimetallic catalyst with enhanced electrocatalytic performances for electro-oxidation and oxygen reduction reactions. *Adv. Funct. Mater.* **2011**, *21*, 4364–4370. [CrossRef]

88. Xiong, L.; Huang, Y.X.; Liu, X.W.; Sheng, G.P.; Li, W.W.; Yu, H.Q. Three-dimensional bimetallic Pd–Cu nanodendrites with superior electrochemical performance for oxygen reduction reaction. *Electrochimica Acta* **2013**, *89*, 24–28. [CrossRef]